Egyptian Journal of Chemistry

http://ejchem.journals.ekb.eg/

Treatment of industrial wastewater containing copper and lead ions using new carboxymethyl chitosan-activated carbon derivatives

Osama Abdel Hafez[1], Riham R. Mohamed[1], Maram T.H.A. Kana[2], Eslam A. Mohamed[3], Nabel A. Negm[3*]

1- Department of Chemistry, Faculty of Science, Cairo University, Giza, 12613, Egypt.

2- National Institute of Laser Enhanced Sciences, Cairo University, Giza, Egypt.

3- Egyptian Petroleum Research Institute, Cairo, Egypt.

Abstract

New carboxymethyl chitosan-activated carbon derivatives were synthesized and characterized using FTIR, XRD and SEM spectra. The prepared adsorbents were containing different ratios of activated carbon ranged between 5% and 20% relative to the carboxymethyl chitosan. The prepared adsorbents were evaluated as adsorbents for removal of copper and lead ions from industrial wastewater. The efficiency of the removal was increased by increasing the percentage of activated carbon in the adsorbent. The adsorption process of the two metals on the synthesized adsorbents was followed Langmuir adsorption isotherm with correlation coefficients R^2 ranged from 0.999 to 1, and follows also the pseudo second order kinetic model. The highest adsorption efficiency was obtained in the alkaline medium using the higher activated carbon content in the adsorbent and was 95.8% for Pb^{2+} and 95.9% for Cu^{2+} after 6 h.

Keywords: Chitosan; industrial waste water; adsorption efficiency; Langmuir.

1. Introduction

Heavy metal water pollution is the contamination of water in natural resources by heavy metals [1]. Traditional treatment methods including: chemical precipitation [2], electrochemical deposition [3], ion exchange, and membrane separation [4] have been applied. Adsorption method using natural biosorbents is alternative to these methods. Numerous studies have demonstrated the effectiveness of chitosan and derived products in the uptake of metal cations such as lead, cadmium, copper, and nickel and the uptake of oxyanions as well as complexed metal ions [5–7]. Chitosan is undoubtedly one of the most popular adsorbents for metal ions removal from aqueous solution and is widely used in waste treatment applications [8]. The binding ability of chitosan for metal cations is mainly due to the amine groups (–NH_2) on the chitosan chain which can serve as coordination sites for many metals. The extent of metal adsorption depends on the source of chitosan [9], the degree of deacetylation [10], the nature of the metal ion [11], and solution conditions such as pH [12]. In spite of its prolific use, the adsorption ability of chitosan has not been realized to a satisfying level. In recent years, attention focused on several adsorbents which have metal-binding capacities and high selectivity to remove heavy metals from contaminated water [13]. In order to improve the sorption selectivity and adsorption ability of chitosan for metal ions, a great number of chitosan derivatives have been prepared by grafting new functional groups such as histidine [14], heparin [15], succinic anhydride [16], N,O-carboxymethyl [17] through a cross-linked chitosan back bone. Further, chemical modifications of chitosan were made to improve the selectivity and the capacities towards heavy metal ions [18]. Substituted chitosan was prepared and regarded as a simple and effective process to facilitate the adsorption ability of chitosan with heavy metals. In the present study, carboxymethyl chitosan-activated carbon derivatives were synthesized and evaluated as adsorbents for removal of copper and

lead ions from industrial wastewater. In the present work, new carboxymethyl chitosan-activated carbon derivatives were synthesized, characterized using FTIR, XRD and SEM spectra and evaluated as adsorbents for removal of copper and lead ions from industrial wastewater.
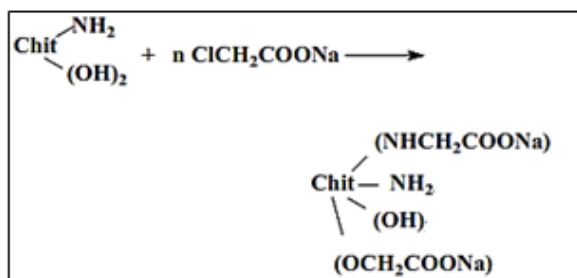
2. Experimental techniques

2.1 Materials

$CuSO_4$, $Pb(CH_3COO)_2$ and NH_4OH were purchased from ADWIC chemicals company, Egypt. The transition metals solutions were prepared by dissolving known weight of $CuSO_4$ and $Pb(CH_3COO)_2$ salts in double distilled water.

2.2 Synthesis

2.2.1 Preparation of carboxymethyl chitosan

O, N-carboxymethyl chitosan was synthesized by the method reported [19]: Carboxymethyl chitosan was prepared by treatment of 20 g chitosan suspended in 1000 mL isopropanol with 27 g sodium hydroxide in a three-necked flask equipped with a condenser, under stirring at room temperature for one hour. Thereafter, chloroacetic acid (30 g in 20 mL isopropanol) was added into the reaction mixture in six equal portions over a period of 30 min, followed by raising temperature to 60 oC and allowed to continue for 2 h. Finally, the resultant solution was filtered and the filter cake was rinsed with 80% aqueous methanol and dried over night at room temperature, followed by estimation of nitrogen and carboxylic contents, *Scheme 1*.

Scheme 1: Synthetic procedures of carboxymethyl chitosan.

2.2.2 Preparation of activated carbon

The collected date palm leaves were rinsed thoroughly with distilled water, dried and then crushed into small fragments. The obtained fragments were steeped in a sulfuric acid solution (25%) for 24 h at 25°C as descried [20]. The treated fragments were rinsed thoroughly with deionized water and air dried. Next, the dried samples were calcined at 250°C in a muffle furnace for 24h. The obtained activated carbon samples were washed several times with deionized water then with sodium bicarbonate solution (1%) until the pH became steady at a value around 6.0. Eventually, the acquired activated carbon samples were dried at 100 °C overnight, grinded and finally sieved.

2.2.3 Preparation of adsorbents

The targeted adsorbents were prepared by physical mixing of the synthesized carboxymethyl chitosan and activated carbon. The ratio between the carboxymethyl chitosan to activated carbon was 95-5 (CMCH-AC 95-5), 90-10 (CMCH-AC 90-10), and 80-20% (CMCH-AC 80-20), respectively. The components were mixed in ball-mill grinder for 30 minutes.

2.3 Adsorption study

Copper (II) and lead (II) solutions were prepared by dissolving 0.25 gL^{-1} of $CuSO_4.2H_2O$ and $Pb(Ac)_2$ in deionized water. For each experiment, 0.5 g of each adsorbent was added in 100 mL of metal solution (250 ppm) in 250 mL Erlenmeyer flask. The flasks were stirred at 150 rpm for different time intervals of: 20, 40, 60, 80, and 100 min at 25 °C. After the treatment, adsorbents were separated by vacuum filtration. Several experiments were conducted to evaluate the effect of pH on adsorption at neutral and alkaline medium (7 and 10) at 250 ppm solution of the different metals. Values of pH were adjusted by adding few drops of NH_4OH or HCl solutions [11]. The residual metal concentrations remained in solutions after treatments were determined by atomic absorption spectroscopy (AAS).

2.4 Data processing

The obtained data from adsorption experiments were analyzed using different adsorption isotherms.

The percent removal (η %) and the equilibrium adsorption capacity qe (mg g^{-1}) of M(II) in solutions were calculated using the following equations:

$$\eta\% = \frac{C_o - C_e}{C_0} \times 100$$

$$q_e = (C_0 - C_e)\frac{V}{M}$$

where: C_e: concentration of adsorbed metal ions at equilibrium (mg L^{-1}), C_o: initial concentration of metal ions in the solution (mg L^{-1}), V: volume of solution (L), M: weight of used adsorbent (g), η%: efficiency of adsorbent in metal adsorption process, and q_e: amount of metals adsorbed by 1 g of adsorbent at equilibrium (mg g^{-1}).

3. Results and Discussion

3.1 Structure of adsorbents

The FTIR spectra of activated carbon samples of date palm leaves are shown in **Figure 3**. These spectra show abroad stretching vibrational band of hydroxyl (–OH) at about 3400 cm^{-1}, vibrational bands of aliphatic C–H at 2926 cm^{-1}, stretching vibrational band of carboxyl group (C=O) in carboxylic acid or quinone type structure at 1710 cm^{-1}, stretching vibrational bands of C=O (–COO−) or C=C centering at 1616 cm^{-1}, bending vibrational band of C–H at 1442 cm^{-1} [21]. Vibrational bands at 1105, 800, and 473 cm^{-1} are the normal vibration modes of the SO_4^{2-} tetrahedral configuration [22]. Since the bands at 3400, 2926, and 1713 cm^{-1} are ascribable to ν(O–H), ν(C–H) and ν(C=O) vibrations, this suggests that date palm leaves were oxidized by sulfuric acid [20].
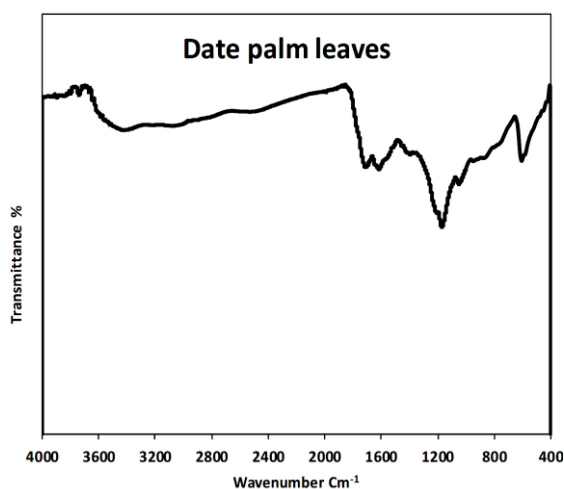

Figure 1: FTIR spectra of activated carbon samples of date palm leaves.

The SEM images of the activated carbon samples derived from date palm leaves are shown in **Figure 2**. It can be observed that the samples of activated carbon particles have a rough surface with several large pores and cracks on their surface. The existence of these pores is attributed to release of volatile organic and inorganic compounds during the activation process using sulfuric acid.
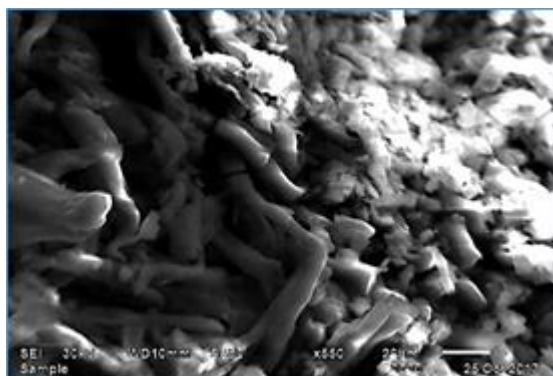

Figure 2: SEM images of activated carbon.

The chemical structure of the prepred carboxy methyl chitosan was determined by FTIR spectra which showed the characteristic absorptin bands at: NH_2 stretching band at 3425 cm^{-1},

2870–2920 cm^{-1} for C-H stretching, 1026 cm^{-1} attributed for the skeletal vibration of C-O-C, CH_2–bending appeared at 1420 cm^{-1}, the asymmetric stretching of C-O-C bridge around 1153 cm^{-1}, amide C=O streching found at 1318 cm^{-1}, 895 cm^{-1} C-O-C bridge as well as glucosidic linkage [23].

XRD profile of the prepared adsorbents were identical to each other with a characteristic peat at 2θ=19.5°, which indicates the semicrystalline structure of the biopolymer, and also large noncrystalline regions through the polymer framework (**Figure 3**).

The diffraction angle near to 2θ = 20° is a characteristic for chitosan framework [24]. The shoulder and the secondary stretch at 26.6°(101) and 43.5° characterize the graphitic carbon card (75–1621, JCPDS card). This illustrates the efficient miximg (milling) of the two adsorbent components [25].
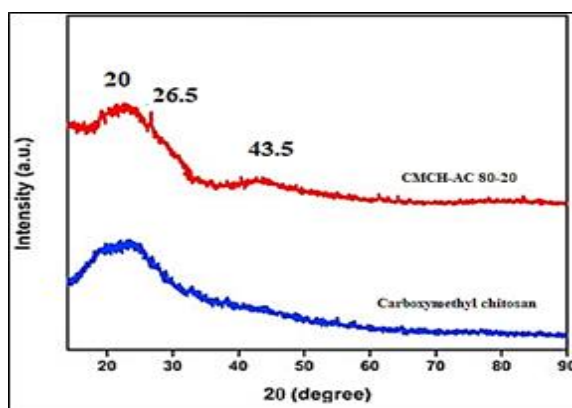

Figure 3: XRD profile of carboxymethyl chitosan and the prepared adsorbents (representatively for CMCH-AC 80-20)
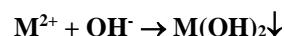
3.2 Adsorption capacity of adsorbents

The amounts of adsorbed metals on different adsorbents were determined by determining the remaining amounts of dissolved metal ions in the solutions after adsorption processes. The values of remaining metal ions in solutions after treatment with different adsorbents are listed in **Table 1**.

Data in **Table 1** represent the concentrations of metal ions remained in the solutions and adsorption efficiency (η %) of adsorbents. It is clear that the concentration of metal ions decreased gradually by the gradual increase of immersion time. The highest adsorption efficiency was obtained in presence of CMCH-AC 80-20. The maximum efficiency is reached 95.8% and 95.9% in case of CMCH-AC 80-20 in presence of both Pb(II) and Cu(II) metal ions in alkaline medium (pH=10). In neutral medium (pH=7), the adsorption efficiency is reached 51.3% and 71.0%, respectively.

The adsorption efficiency of CMCH-AC 90-10 adsorbent depressed to 90.3% and 94.3% in presence of Pb(II) and Cu(II) in alkaline medium (pH=10). In neutral medium (pH=7), the depression in adsorption efficiency reached to 48.6% and 63.2% in case of Pb(II) and Cu(II) metal ions, respectively.

The adsorption efficiency of CMCH-AC 95-5 adsorbent had similar trend for Pb(II) and Cu(II) metal ions. In case of alkaline medium, the adsorption efficiency of Pb(II) and Cu(II) reached to 63.5% and 78.2%, respectively. While, changing pH to alkaline (pH=7) decreased the adsorption efficiency to 36.7% and 62.7%, respectively.

It is clear from the data obtained in *Table 1* that, the adsorption process of metal ions in alkaline medium is more efficient than that occurred in neutral medium. Also, the adsorption of copper ions is more pronounced than lead ions. The pronouncement of adsorption in alkaline medium can be attributed to the precipitation of metal ions in the form of insoluble hydroxides, as represented in the following equation:

$$M^{2+} + OH^- \rightarrow M(OH)_2\downarrow$$

Copper and lead ions are highly sensitive towards the alkalinity of the medium [26]. Depending on pH of the medium, Cu(II) and Pb(II) ions start to precipitate at pH=8-10, and reached to complete precipitation at pH=12. In pH=10, the ionic species of Cu(II) and Pb(II) start to change to hydroxide form, as a result, the medium contains both hydroxide form and ionic form of the metal ions. That decreases the metal ion amounts in the solution, and consequently the efficiency of metal removal increased [27]. The formed hydroxides precipitate in the network of the biopolymers according to intraparticle model. The ions in the In neutral medium, the ionic species of Cu(II) and Pb(II) remains in their ionic forms.

The data listed in *Table 1* showed acceptable adsorption efficiency for chitosan and its modified forms in Cu(II) and Pb(II) removal from wastewater by adjusting the pH of the medium to a suitable values
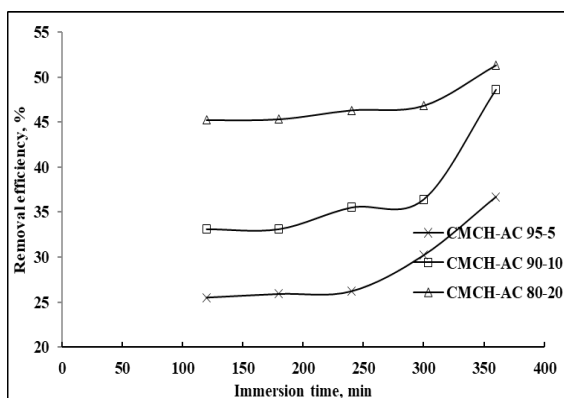
Table 1: Equilibrium concentration (C_e) and removal efficiency (η %) of Pb(II) and Cu(II) in presence of chitosan and chitosan modified adsorbents

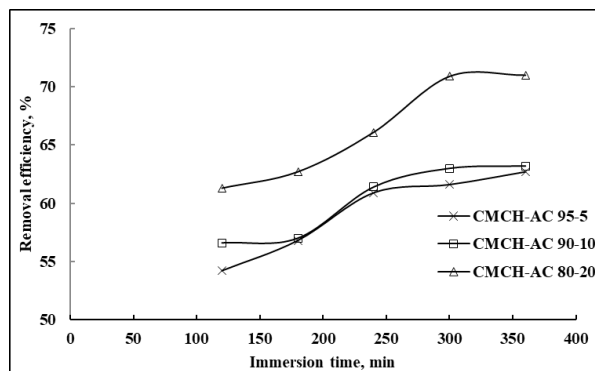| Adsorbents Chitosan-activated carbon	t (min)	Pb (pH 7)		Pb (pH 10)		Cu (pH 7)		Cu (pH 10)	
		C_e, (mg L^{-1})	η %	C_e, (mg L^{-1})	η %	C_e, (mg L^{-1})	η %	C_e, (mg L^{-1})	η %
CMCH-AC 95-5	120	176.2	25.5	89.0	60.5	104.4	54.2	52.4	75.0
	180	175.2	25.9	88.8	60.6	98.0	56.8	52.3	75.1
	240	174.5	26.2	87.3	61.1	87.8	60.9	52.1	75.1
	300	164.4	30.2	83.8	62.6	85.9	61.6	48.4	76.7
	360	148.2	36.7	81.4	63.5	83.3	62.7	44.4	78.2
CMCH-AC 90-10	120	157.3	33.1	84.5	62.2	98.4	56.6	11.7	91.3
	180	157.2	33.1	78.3	64.7	97.4	57.0	11.5	91.4
	240	151.3	35.5	49.5	76.3	86.6	61.4	5.6	93.8
	300	148.9	36.4	17.0	89.2	82.6	63.0	4.5	94.3
	360	118.7	48.6	14.3	90.3	82.0	63.2	4.1	94.3
CMCH-AC 80-20	120	126.9	45.2	1.9	95.2	87.2	61.3	1.6	95.3
	180	126.9	45.3	1.7	95.3	83.2	62.7	1.6	95.4
	240	124.3	46.3	0.8	95.7	74.7	66.1	1.5	95.4
	300	123.2	46.8	0.7	95.8	62.7	70.9	0.8	95.7
	360	111.6	51.3	0.6	95.8	62.7	71.0	0.3	95.9

3.3 Effect of contact time

The contact time defined as the time of immersing the adsorbents in the metal ion solution. The influence of adsorbents towards the immersion time is determined by the stability of the metal complex formed during the adsorption process between the metal ions and the adsorbents [28]. Highly stable metal/adsorbent complexes associated by high metal adsorption efficiency, while low stable metal/ adsorbent complexes dissociated in the medium, and consequently decreases the adsorption efficiency by time.
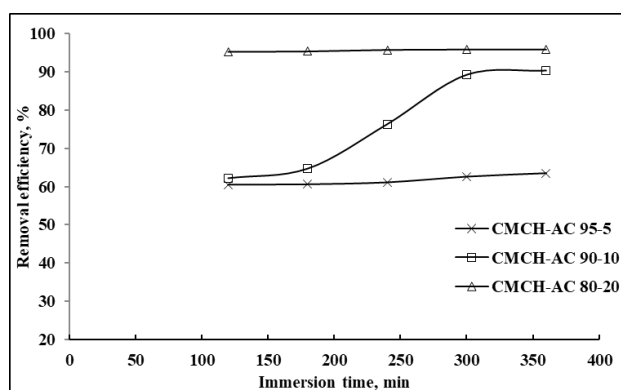
For copper complexes in neutral and alkaline medium, the removal percent was decreased by increasing the immersion time of the adsorbents. That can be attributed to the weak complexation tendency of copper ions and the different adsorbents. *Table 1* showed that the concentration of lead ions decreased considerably in the initial time of adsorption process (t=120 min). In case of copper ions, the formed complexes between copper ions and CMCH-AC 80-20 and CMCH-AC 90-10 adsorbents are stable complexes. That is due to the presence of several adsorption sites in the framework of the prepared adsorbents. These adsorption sites are from the carboxymethyl chitosan biopolymer and the activated carbon. Increasing the ratio of the activated carbon increases the adsorption efficiency, which can be attributed to the presence of different varieties of functional groups in the activated carbon than the carboxymethyl chitosan, *Figure 4a-d*. While in case of CMCH-AC 95-5 adsorbent, the main adsorption sites are the hydroxyl and amino groups, which could be shielded due to the segments conflict and consequently decreases their efficiency of adsorption.
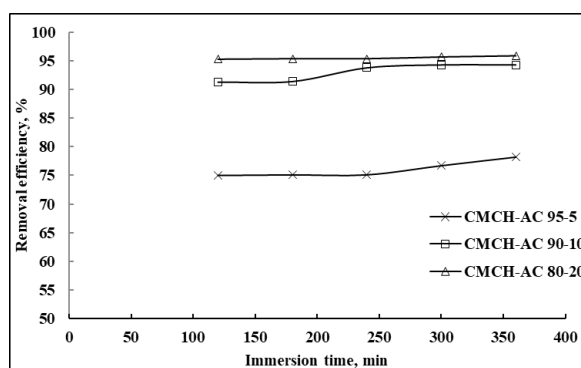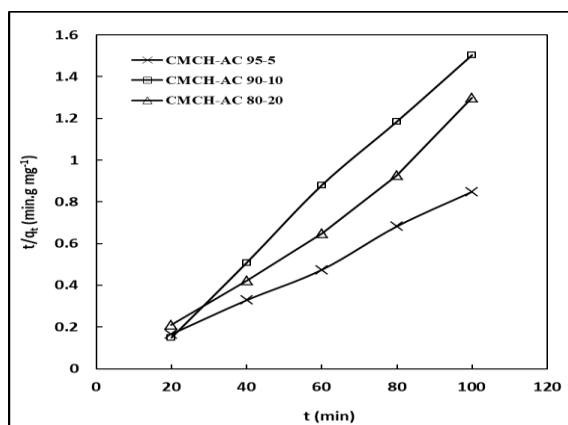
(b)

(c)

(d)

Figure 4: Effect of immersion time on the adsorption efficiency of the prepared adsorbents for (a) Pb^{2+} (pH 7), (b) Cu^{2+} (pH 7), (c) Pb^{2+} (pH 10), and Cu^{2+} (pH 10) at 25 ºC.
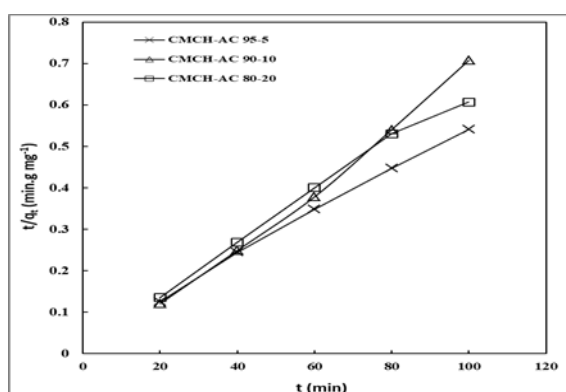
3.4 Adsorption kinetics

The kinetic parameters were studied using 250 ppm of Cu(II) and Pb(II) in pH 7 and 10, in presence of 0.5 gL^{-1} adsorbent, at 25 °C. The remained concentrations of Cu(II) and Pb(II) were analyzed during time intervals of: 20-100 min during the adsorption process. The obtained data were processed

(a)

using several adsorption models including: pseudo first order kinetic, pseudo second order kinetic, first order reversible reaction model and intraparticle diffusion model [29]. These models describe the adsorption of transition metal ions onto the different adsorbents. The data were fitted according to the pseudo second order kinetics and the intraparticle diffusion model as potential models for the behavior of Cu(II) and Pb(II) adsorption.

Table 2 represents the obtained adsorption kinetic parameters of pseudo second order kinetic model. The correlation coefficients (R^2) were around unity, which indicates that the adsorption of Cu(II) and Pb(II) metal ions on the different adsorbents follow the pseudo second order rate expression. That indicates the adsorption of the tested metal ions on the different adsorbents depends on both the concentration of the metal ion and also the amount of the used adsorbents [30].
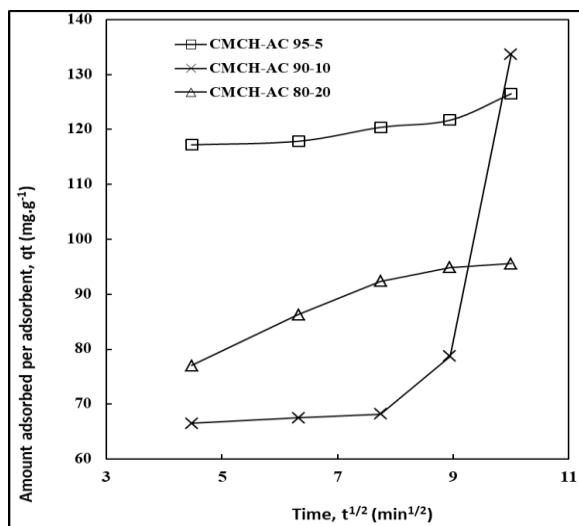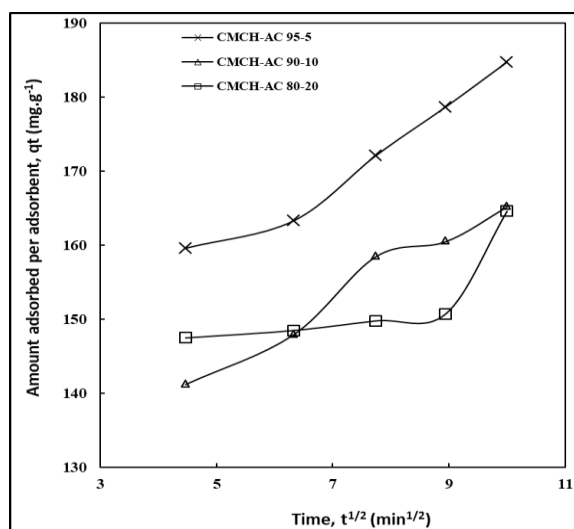
The intraparticle diffusion model commonly divides the adsorption process into three stages: the rapid surface adsorption stage, the gradual inward diffusion stage and the final equilibrium stage. Plotting the adsorption capacity (q_t) verses square root of adsorption time ($t^{1/2}$) gave characteristic curves with three periods. These periods are attributed to the adsorption stages of the exterior surface, interior surface, and equilibrium, respectively, as shown in *Figure 5*.

(a)

(a)

(b)

Figure 5: Pseudo second order profile for: (a) Pb(II), and (b) Cu(II) adsorption on the synthesized adsorbents.

(b)

Figure 6: Interparticle diffusion profile of adsorption of (a) Cu(II), and Pb(II) ions on the synthesized adsorbents at 25 ºC.

Interparticle diffusion model describes three stages of metal adsorption process by adsorbents. In the first stage, adsorption takes place on exterior surface of adsorbent until the exterior surface is saturated by metal ions. The second stage takes place by entering the adsorbed metal ions into pores of adsorbents within the particle. When the metal ions diffused into adsorbent pores, the diffusion resistance increased due to crowding, and consequently the diffusion rate decrease. The third stage is the equilibrium between the metal ions in the solution and the adsorbed ions. This stage is very slow due to the decrease of metal ions concentration in the solution. Inspection of *Figure 6a,b* showed two different characteristics for Pb(II) and Cu(II) metal ions adsorption. In case of Pb(II)metal ions, it is clear that the adsorption in the first stage occurred in fast step. That leads to saturation of the adsorbent surface, and then the rate of adsorption decreases considerably. The third step occurred at longer time with very small rate. The gradual decrease in the adsorption capacity of the adsorbent at the third stage indicates the desorption of Pb(II) ions to the medium. Desorption of Pb(II) ions indicates the weak bond between the adsorbent and the metal ions. That behavior is inverted in case of Cu(II) ions adsorption. The adsorption capacity increased gradually by time, indicating the successive adsorption of Cu(II) ions on the adsorbent surface. That indicates the strong bond formed between the synthesized adsorbents and Pb(II) and Cu(II) metal ions [31]. The intercepts (C) in *Table 3* are not equal to zero, which indicates that the intraparticle diffusion model is the controlling model to determine the kinetics of the adsorption process [2].
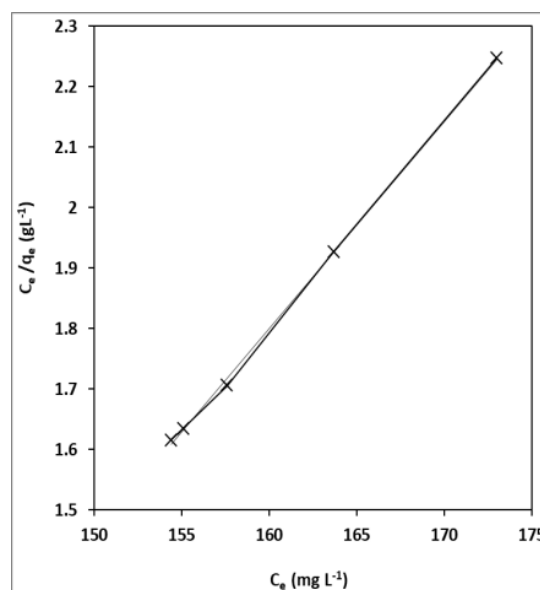
Table 3: Interparticle diffusion model parameters

of Pb(II) and Cu(II)

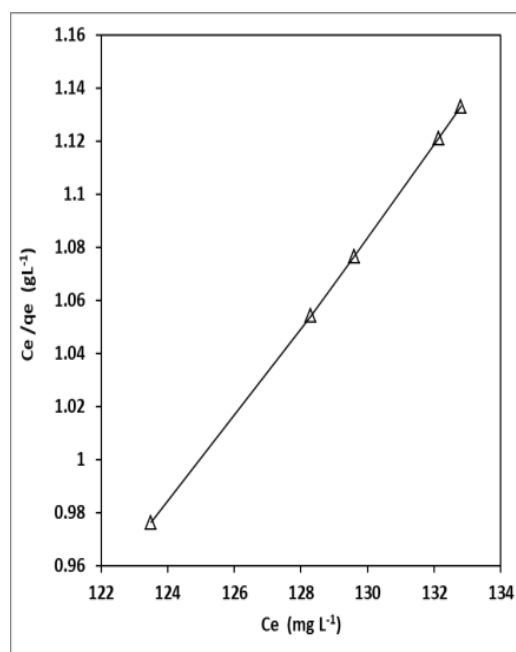| Adsorbent	Pb(II)		Cu(II)	
	K_i (mg g^{-1}min$^{-1/2}$)	C	(mgg^{-1}min$^{-1/2}$)	C
CMCH-AC 95-5	0.07	12.89	0.18	23.36
CMCH-AC 90-10	0.44	47.63	0.20	23.61
CMCH-AC 80-20	0.60	79.88	0.24	28.65

3.5 Adsorption isotherms

There are several adsorption isotherms and models describe the adsorption of metal ions on the different adsorbent systems. These are: Freundlich isotherm, Brunauer–Emmer–Teller (BET) model, Halsey isotherm, Flory–Huggins isotherm, Temkin isotherm, and Langmuir isotherm. Calculation of adsorption data using several models and isotherms revealed that

the system under investigation obeys Langmuir adsorption isotherm. Langmuir isotherm was used to analyze the adsorption equilibrium data of Pb(II) and Cu(II) metal ions on the targeted adsorbents. Langmuir adsorption isotherm describes the adsorption of metal ions on the adsorbents as monolayer, and that adsorption takes place at specific homogeneous sites [32]. Linear plots of Langmuir adsorption isotherm are shown in *Figure 7*. Adsorption isotherm constants for Langmuir model determined in this work are given in *Table 4.*

Pb(II) CMCH-AC 95-5
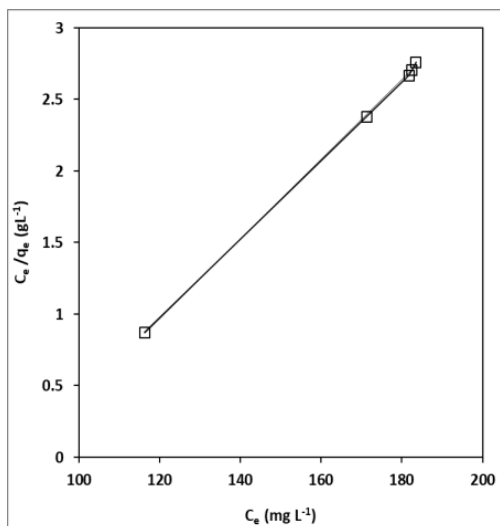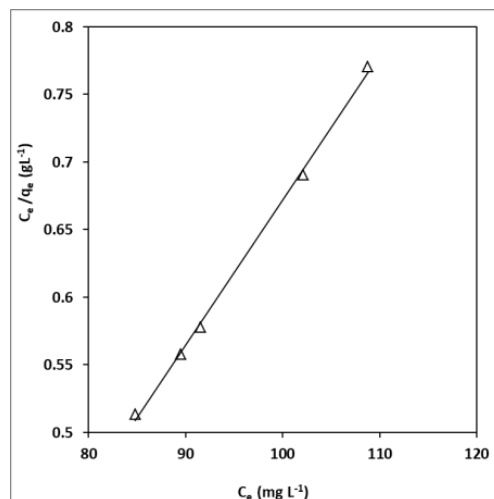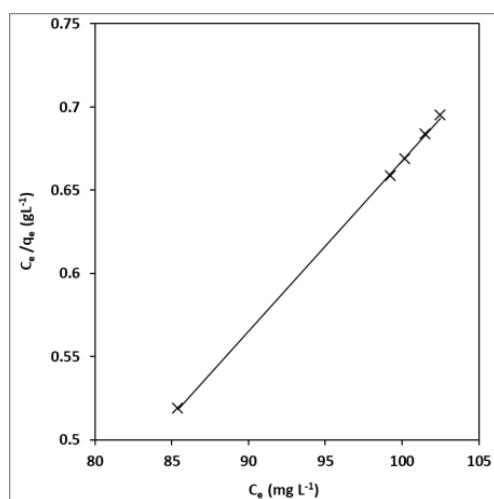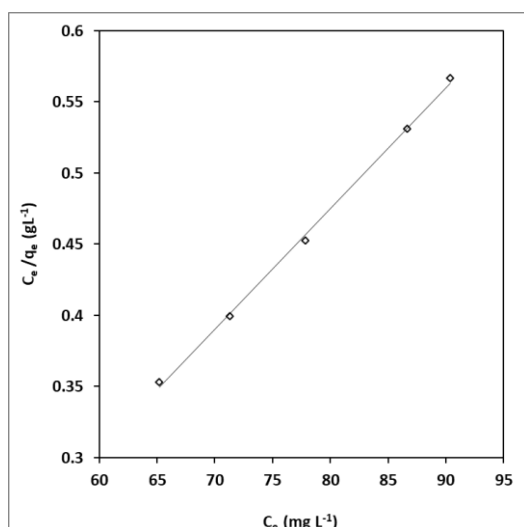

Pb(II) CMCH-AC 90-10

Pb(II) CMCH-AC 80-20

Cu(II) CMCH-AC 80-20

Figure 7: Langmuir adsorption isotherm presentation of Pb(II) and Cu(II) adsorption on the synthesized adsorbents at 25 ºC.

Cu(II) CMCH-AC 95-5

Table 4: Parameters of Langmuir adsorption isotherm

Biosorbent	pH	Metal ions	R^2
CMCH-AC 90-10	**7**	Pb(II)	0.999
		Cu(II)	0.999
	9	Pb(II)	1
		Cu(II)	1
CMCH-AC 80-20	**7**	Pb(II)	0.999
		Cu(II)	0.999
	9	Pb(II)	0.999
		Cu(II)	1
CMCH-AC 95-5	**7**	Pb(II)	0.999
		Cu(II)	0.999
	9	Pb(II)	0.999
		Cu(II)	0.999

It can be seen that the equilibrium data for M(II) adsorption on chitosan and its derivatives fit Langmuir model [31], which indicated that M(II) adsorption on the these adsorbents was a monolayer adsorption process occurring at specific homogeneous sites [33-35]. The Langmuir monolayer adsorption capacities (q_{max}) and the Langmuir equilibrium constant k_L values for chitosan were higher than the values of **CMCH-AC 90-10** and **CMCH-AC 95-5**, indicated that the modification process reveres influenced M(II) adsorption equilibrium.

Cu(II) CMCH-AC 90-10

Conclusion

New carboxymethyl chitosan-activated carbon derivatives were synthesized and evaluated as adsorbents for removal of copper and lead ions from industrial wastewater. The efficiency of the removal was increased by increasing the percentage of activated carbon in the adsorbent. The adsorption process of the two studied metal on the synthesized adsorbents followed Langmuir adsorption isotherm, according to the pseudo second order kinetic model. The highest adsorption efficiency was obtained at the alkaline medium using the higher activated carbon content in the adsorbent.

3. Reference

[1] T. Rasheed, A.A. Hassan, M. Bilal, T. Hussain, K. Rizwan, Metal-organic frameworks based adsorbents: A review from removal perspective of various environmental contaminants from wastewater, Chemosphere. 259 (2020) 127369.

[2] S.A. Mirbagheri, S.N. Hosseini, Pilot plant investigation on petrochemical wastewater treatmentfor the removal of copper and chromium with the objective of reuse, Desalination. 171 (2005) 85–93.

[3] O.C. Engineering, Treatment of nitrobenzene-containing wastewater by iron-carbon micro-electrolysis, 66 (2015).

[4] S. Guida, G. Rubertelli, B. Jefferson, A. Soares, Demonstration of ion exchange technology for phosphorus removal and recovery from municipal wastewater, Chem. Eng. J. 420 (2021) 129913.

[5] N.A. Negm, R. El Sheikh, A.F. El-Farargy, H.H.H. Hefni, M. Bekhit, Treatment of industrial wastewater containing copper and cobalt ions using modified chitosan, J. Ind. Eng. Chem. 21 (2015) 526–534.

[6] S. Fan, J. Chen, C. Fan, G. Chen, S. Liu, H. Zhou, R. Liu, Y. Zhang, H. Hu, Z. Huang, Y. Qin, J. Liang, Fabrication of a CO2-responsive chitosan aerogel as an effective adsorbent for the adsorption and desorption of heavy metal ions, J. Hazard. Mater. 416 (2021) 126225.

[7] M. Rahaman, M. Islam, M. Islam, M. Rahman, S.. Alam, Biodegradable composite adsorbent of modified cellulose and chitosan to remove heavy metal ions from aqueous solution, Curr. Res. Green Sustain. Chem. 4 (2021) 100119.

[8] Y. Liu, L. Hu, B. Tan, J. Li, X. Gao, Y. He, X. Du, W. Zhang, W. Wang, Adsorption behavior of heavy metal ions from aqueous solution onto composite dextran-chitosan macromolecule resin adsorbent, Int. J. Biol. Macromol. 141 (2019) 738–746.

[9] E. Guibal, Interactions of metal ions with chitosan-based sorbents: a review, Sep. Purif. Technol. 38 (2004) 43–74.

[10] M. Benavente, Phd thesys on Chitosan - chelating properties, 2008.

[11] H.A. Abubshait, A.A. Farag, M.A. El-Raouf, N.A. Negm, E.A. Mohamed, Graphene oxide modified thiosemicarbazide nanocomposite as an effective eliminator for heavy metal ions, J. Mol. Liq. (2020) 114790.

[12] A.M. Shehap, R.A. Nasr, M.A. Mahfouz, A.M. Ismail, Preparation and characterizations of high doping chitosan/MMT nanocomposites films for removing iron from ground water, J. Environ. Chem. Eng. 9 (2021) 104700.

[13] H. Zhang, X. Yuan, T. Xiong, H. Wang, L. Jiang, Bioremediation of co-contaminated soil with heavy metals and pesticides: Influence factors, mechanisms and evaluation methods, Chem. Eng. J. 398 (2020) 125657.

[14] G.Z. Kyzas, D.N. Bikiaris, Recent modifications of chitosan for adsorption applications: A critical and systematic review, Mar. Drugs. 13 (2015) 312–337.

[15] W. Wang, Q. Meng, Q. Li, J. Liu, M. Zhou, Z. Jin, K. Zhao, Chitosan derivatives application biomedicine, Int. J. Mol. Sci. 21 (2020).

[16] K.G.P.C. De Mello, L.D.C. Bernusso, R.N.D.M. Pitombo, B. Polakiewicz, Synthesis and physicochemical characterization of chemically modified chitosan by succinic anhydride, Brazilian Arch. Biol. Technol. 49 (2006) 665–668.

[17] O.F. Abdel Gawad, Graft modification of carboxymethyl chitosan with styrene and its biological applications, Beni-Suef Univ. J. Basic Appl. Sci. 9 (2020).

[18] R. El-Sheikh, H.H. Hefni, A.F. El-Farargy, M. Bekhit, N.A. Negm, Adsorption efficiency of chemically modified chitosan towards copper and cobalt ions from industrial waste water, Egypt. J. Chem. 55 (2012) 291–305.

[19] D.C. da Silva Alves, B. Healy, L.A. d. A. Pinto, T.R.S. Cadaval, C.B. Breslin, Recent developments in Chitosan-based adsorbents for the removal of pollutants from aqueous environments, Molecules. 26 (2021).

[20] A.M. Soliman, H.M. Elwy, T. Thiemann, Y. Majedi, F.T. Labata, N.A.F. Al-Rawashdeh, Removal of Pb(II) ions from aqueous solutions by sulphuric acid-treated palm tree leaves, J. Taiwan Inst. Chem. Eng. 58 (2016) 264–273.

[21] E.A. Azmy, H.E. Hashem, E.A. Mohamed,

N.A. Negm, Synthesis, characterization, swelling and antimicrobial efficacies of chemically modified chitosan biopolymer, J. Mol. Liq. 284 (2019) 748–754.

[22] N.A. Negm, G.H. Sayed, F.Z. Yehia, O.I. Habib, E.A. Mohamed, Biodiesel production from one-step heterogeneous catalyzed process of Castor oil and Jatropha oil using novel sulphonated phenyl silane montmorillonite catalyst, J. Mol. Liq. 234 (2017) 157–163.

[23] H.F.G. Barbosa, D.S. Francisco, A.P.G. Ferreira, É.T.G. Cavalheiro, A new look towards the thermal decomposition of chitins and chitosans with different degrees of deacetylation by coupled TG-FTIR, Carbohydr. Polym. 225 (2019) 115232.

[24] M. Eddya, B. Tbib, K. EL-Hami, A comparison of chitosan properties after extraction from shrimp shells by diluted and concentrated acids, Heliyon. 6 (2020) e03486.

[25] K. Rambabu, J. AlYammahi, G. Bharath, A. Thanigaivelan, N. Sivarajasekar, F. Banat, Nano-activated carbon derived from date palm coir waste for efficient sequestration of noxious 2,4-dichlorophenoxyacetic acid herbicide, Chemosphere. 282 (2021) 131103.

[26] T. Wen, F. Qu, N.B. Li, H.Q. Luo, A facile, sensitive, and rapid spectrophotometric method for copper(II) ion detection in aqueous media using polyethyleneimine, Arab. J. Chem. 10 (2017) S1680–S1685.

[27] G.M. Al-Senani, F.F. Al-Fawzan, Adsorption study of heavy metal ions from aqueous solution by nanoparticle of wild herbs, Egypt. J. Aquat. Res. 44 (2018) 187–194.

[28] K.C. Khulbe, T. Matsuura, Removal of heavy metals and pollutants by membrane adsorption techniques, Appl. Water Sci. 8 (2018).

[29] S Dahiya, RM Tripathi, and AG Hegde, Hazard Mater J. 150 (2008) 376.

[30] HK Alluri, SR Ronda, VS Settalluri, JS Bondili, V P Suryanayarana, Venthakeshwar, African J. Biotechnol. 6 (2007) 2924.

[31] S Wang, and E Ariyanto, J. Colloid Interface Sci. 314 (2007) 25.

[32] CW Feng, TR Ling, and JR Shin, J. Environ. Manag. 91 (2010) 798.

[33] MU Dural, L Cavas, SK Papageorgiou, and FK Katsaros, Chem. Eng. J. 168 (2011) 77.

[34] O Gok, A Ozcan, B Erdem, AS Ozcan, Colloids Surf. A: Physicochem. Eng. Aspects 317 (2008) 174.

[35] Y Ren, X Wei, M Zhang, J. Hazard. Mater. 158 (2008) 14.